Broadband Communication Signal Detection Using Deep Convolutional Autoencoder and Spectrum Center Network

Bin Wei
School of Cyberspace Security, Gansu University of Political Science and Law, Lanzhou 730070, China
E-mail: weibin@gsupl.edu.cn

Keywords: deep convolutional autoencoder network, carrier signal detection, signal-to-noise ratio, spectrum center network, broadband power spectrum

Received: February 13, 2025

In the increasingly complex electromagnetic environment, wireless communication technology faces multiple challenges such as noise, interference, multi-path effects, and attenuation, which seriously threaten the reliability and efficiency of communication systems. Therefore, research was conducted on broadband communication signal detection based on deep convolutional autoencoders and spectral center networks. The experiment used a dataset of real-world signals and conducted comprehensive evaluations under various signal-to-noise ratios, signal-to-noise ratios, as well as different code lengths and colored noise backgrounds. The evaluation indicators included computational complexity indicators such as detection accuracy, F1 score, recall rate, specificity, and inference time. The experimental results showed that on the training set, the loss values of convolutional autoencoder networks 1 and 5 decreased rapidly, and their relatively stable loss function values were both around 10^{-5}. The loss value of Convolutional Autoencoder Network 10 decreased the slowest, with a minimum loss function value of about 10-6. Moreover, the method achieved detection accuracy, F1 score, and recall rate of 98.5%, 0.99, and 0.98, respectively, with an average inference time of 0.025 seconds. Compared with the existing state-of-the-art methods, it improved detection accuracy by 13.5% compared to energy detection and 5.3% compared to deep learning detection. The maximum improvement in F1 score and recall was 0.11 and 0.16, respectively. The research results indicated that the proposed method was significantly superior to existing methods in complex electromagnetic environments, with higher detection accuracy and robustness. This method offers insights for the design, technology, and solutions of future communication systems, which helps to promote the continuous development and progress of communication technology.

Povzetek: Članek uvaja metodo zaznavanja širokopasovnih komunikacijskih signalov z uporabo globokega konvolucijskega avtoenkoderja in spektralnega omrežja za natančno oceno šumskega dna ter izboljšano robustnost pri nizkem SNR.

1 Introduction

In modern communication systems, signal detection is a crucial step in the receiving process, responsible for identifying and extracting useful information from noise and interference. Its accuracy and efficiency directly affect the quality and reliability of information transmission [1, 2]. In complex electromagnetic environments, communication signal detection faces challenges such as noise, interference, and multi-path effects. Especially under low signal-to-noise ratio conditions, existing methods are difficult to meet the requirements of high accuracy and robustness [3]. Conventional approaches exhibit inadequate accuracy when dealing with low signal-to-noise ratios, coupled with high computational complexity and subpar real-time performance. Alternatively, they may only achieve satisfactory results under very specific circumstances [4, 5]. The powerful feature extraction and pattern recognition capabilities of Deep Learning (DL) provide new ideas for communication signal detection. Convolutional Autoencoder (CAE), as a type of DL model, can effectively learn high-level feature representations from data. Spectrum Center Network (SCN) is an end-to-end CNN model used for carrier signal detection in broadband power spectra. Therefore, a broadband communication signal detection method based on Deep Convolutional Autoencoder (DCAE) and SCN has been proposed to achieve noise floor estimation and carrier signal detection by capturing multi-level features of the signal and dynamically adjusting the feature response. The innovation of this research lies in the formulation of a broadband communication signal detection method grounded in DCAE. This method enables the efficient extraction of pertinent information from complex signals. Furthermore, the investigation into the dynamic embedding of excitation and compression network modules subsequent to convolutional layers, aimed at dynamically modulating the feature response of each channel, serves to augment the network's representational prowess. The significance of the research lies in providing new theoretical and technological foundations for future research in the field of communication signal detection, which helps to promote further development in related fields.

2 Related works

As communication technology evolves, the characteristics of signal modulation, transmission rate, and bandwidth are also constantly changing. These changes require signal detection technology to adapt to different signal characteristics and achieve accurate detection of various signals. To fulfill the detection needs of faint broadband communication signals, Xiao L proposed a random resonance signal detection approach grounded on local spectrum of broadband signals for small unmanned aerial vehicle reconnaissance and communication scenarios. The research outcomes indicated that in comparison with traditional methods, this method optimized performance by about 6 db. For lower signal-to-noise ratio (SNR) situations, a dual channel collaborative detection method combining random resonance and cross-correlation detection was proposed to further improve detection performance [6].

Jiang X proposed a new signal detection algorithm to optimize the accurate detection of signals in satellite communication systems and reduce inter signal interference. The algorithm utilizes stochastic resonance technology to enhance the SNR of input signals and combines energy detection and dual thresholding for accurate judgment. The test outcomes demonstrated that the algorithm could validly detect signals under low SNR conditions, improving the performance of the entire satellite communication system [7]. Li S proposed a method based on Quadrature Amplitude Modulation-Orthogonal Frequency Division Multiplexing (QAM-OFDM) echo to construct a Constructed Step Linear Frequency Modulated (CStep-LFM) signal for detecting weak targets in integrated radar communication signals. The research results indicated that when compared to various existing integrated signals, the CStep-LFM signal not only enhanced the detection capability for weak targets but also exhibited superior communication performance [8]. Chen Y proposed a novel detector considering a random flow model to investigate the impact of environmental signal source flow on the detection performance of backscatter communication systems. The research results indicated that random source traffic could significantly degrade the performance of existing detectors, resulting in an error plateau at low SNRs. The new detector could significantly improve the detection performance in the presence of source traffic by weighting samples. The gain could exceed 3db in some cases, but as the SNR increased and the sample size decreased, the gain might turn negative due to the use of heuristic detection thresholds [9].

DL technology has yielded notable outcomes in areas like image recognition and speech processing, and its potent capabilities in feature extraction and pattern recognition offer fresh perspectives for detecting communication signals. To improve the performance of underwater acoustic communication preamble signal detection and cope with complex channel environments, Liu Z proposed a compact neural network grounded on Lenet-5, which adopts deep separable convolution and global average pooling techniques, and combines filter pruning and post training quantization techniques to enhance network compression further. The research outcomes indicated that the detection ability of this lightweight neural network was close to that of classical Convolutional Neural Networks (CNNs), and the parameters and computational complexity were considerably decreased, meeting the requirements of timeliness and low power consumption for underwater acoustic communication [10]. Arya S proposed a novel statistical model based on the assumption of single scattering to improve the fault-tolerant cooperative signal detection performance of short-range optical terahertz wireless communication. The research results indicated that when using the optimal voting rule and a given target bit error rate, the number of collaborative users required by the network was less than the overall user count in the optical network [11].

In summary, many scholars have conducted research on communication signal detection and achieved certain results. Comparing the performance of different methods in terms of detection accuracy, SNR performance, and computational efficiency, it can be seen that although the ED method had low computational complexity, its detection accuracy was poor under low SNR conditions, making it difficult to effectively distinguish between signal and noise. Its detection accuracy was 85%, SNR was 1db, and inference time was 0.015 seconds. Although the DLD method had a high detection accuracy of 93.2%, it had high computational complexity, a long inference time of 0.03 seconds, high hardware resource requirements, and an SNR of 0db. The stochastic resonance detection method performed well under low SNR conditions, with an SNR of -6 db, but had high computational complexity and limited adaptability, with a detection accuracy of 90% and inference time of 0.02 seconds. The QAM-OFDM method was suitable for radar communication integrated signals, with a high detection accuracy of 92%, an SNR of -10 db, and an inference time of 0.025 seconds. However, its robustness to noise and interference was poor. Although the compact neural network based on Lenet-5 had fewer parameters, high computational efficiency (inference time of 0.02 seconds), detection accuracy of 94%, and SNR of -5 db, its adaptability to complex channel environments was limited. However, these existing methods still have limitations in their performance in complex electromagnetic environments, especially under low SNR and high interference conditions. In contrast, the communication signal detection method based on DCAE proposed in the study achieved noise floor estimation and carrier signal detection by processing the signal power spectrum through convolutional and deconvolution layers, and dynamically embedded excitation and squeezing network modules after the convolutional layer, thereby improving the detection accuracy and robustness in complex electromagnetic environments, providing an effective solution for communication signal detection in complex electromagnetic environments.

3 Methods and materials

3.1 Signal noise floor estimation based on DCAE

Communication signal detection refers to identifying and determining whether there is an expected signal from the received signal. This process is the first step in determining whether the communication system can successfully receive information and whether the information can be accurately separated from noise. Communication signals are transmitted through information transmission systems [12]. In the field of communication, the information transmission system model is a fundamental framework for describing the process of information transmission from the sender to the receiver. This model covers multiple key aspects of information encoding, modulation, transmission, reception, and demodulation, and is the foundation for understanding and designing communication systems. Its structure is shown in Fig. 1.

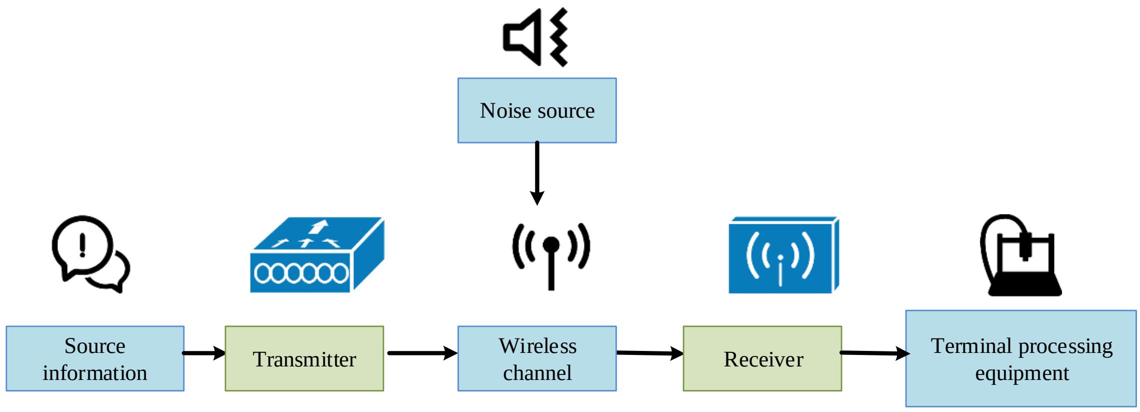

Figure 1: Diagrammatic representation of the information transmission system model

In Fig. 1, the model describes the transmission process of information from the source to the terminal processing device. The source information, as the starting point of the information transmission system, contains the content to be transmitted. The transmitter is responsible for converting the source information into a form suitable for transmission in the channel. This may include signal modulation, amplification, and other processing to ensure that the signal can effectively pass through the channel. Wireless channel is a medium for signal transmission, which can be in wired or wireless form. In wireless channels, signals may be affected by various interferences and noise sources, which can affect the transmission quality of the signal. The receiver is located at the other end of the channel, and its function is opposite to that of the transmitter, responsible for extracting the original information from the received signal. This may include signal demodulation, filtering, and other processing. The terminal processing device is the endpoint of information transmission, responsible for further processing of the information output by the receiver, such as decoding, display, etc., for use by the end user. The communication system model provides a fundamental framework for understanding the transmission characteristics of signals in complex electromagnetic environments, covering the entire transmission process from the source to the terminal processing equipment. The noise introduced by wireless channels in communication system models is one of the key factors affecting signal transmission quality. The DCAE method can effectively estimate the noise floor by learning the feature representation of the signal, thereby improving the accuracy and robustness of signal detection. This process simulates the transmission of signals in wireless channels, especially the signal changes under the influence of noise and interference. To quantify the effective transmission efficiency of signals in complex electromagnetic environments, the amount of information transmitted in a single target selection is calculated, as shown in equation (1).

$$B = \log_2 N + P\log_2 P + (1-P)\log_2\left(\frac{1-P}{N-1}\right) \quad (1)$$

In equation (1), B is the bit rate. N is the number of optional targets. P is the accuracy of target recognition. This indicator reflects the accuracy and reliability of signal detection and recognition under noise interference. Estimating the broadband noise floor is a crucial area of focus within signal processing technology, which directly affects the efficiency of signal detection, especially in broadband carrier detection. CNN represents a type of feedforward neural network characterized by convolutional computations and a deep architecture. It stands as one of the emblematic algorithms in the realm of DL. CAE is a variant of autoencoder that can learn how to recover the original input from contaminated input [13, 14]. Its main goal is to learn higher-level features of input data, rather than relying on details. Therefore, the study proposes a broadband noise floor estimation method based on DCAE by combining the two. DCAE uses convolutional and deconvolution layers to replace fully connected layers in autoencoders. The convolutional layer extracts local features of the input signal, captures noise patterns and structures, and generates abstract feature representations. The deconvolution layer reconstructs the noise base based on these features and generates a noise estimate with the same size as the original input. This structure enables DCAE to recover the original input from contaminated signals and separate the signal from noise. Combining the two-dimensional data processing capability of CNN can improve the accuracy of DCAE noise floor estimation and enhance the robustness of the model. The diagrammatic representation of its structure is in Fig. 2.

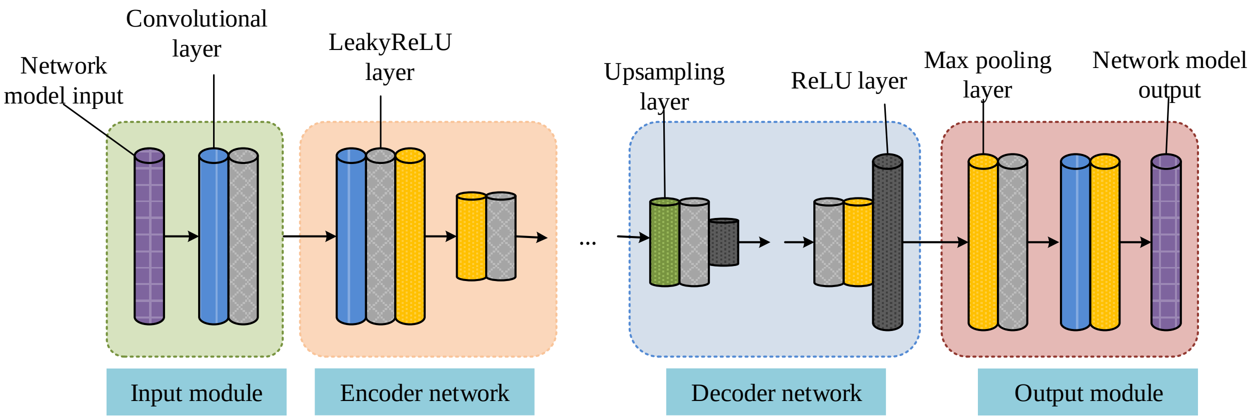

Fig. 2. Schematic representation of the one-dimensional DCAE structure

As depicted in Fig. 2, the DCAE network typically comprises two components: an encoder and a decoder. The encoder, made up of convolutional and pooling layers, is tasked with compressing the input data into a lower-dimensional hidden representation. Conversely, the decoder, which includes a deconvolutional layer, reconstructs the original data from this hidden representation. The encoding process usually involves mapping the input data [15]. The specific calculation is shown in equation (2).

$$z = f(Wx + b) \quad (2)$$

In equation (2), z represents a low dimensional latent space. x is input data. W is the weight matrix (WM). b is a bias vector. f is the activation function (AF). The decoding process usually involves reconstructing the original data. The detailed computation is illustrated in equation (3).

$$\hat{x} = g(W'z + b') \quad (3)$$

In equation (3), $\hat{x}$ is the reconstructed output data. g is the AF. W' is the WM for the decoder. b' is the bias vector for the decoder. The accuracy of noise floor estimation determines the accuracy and efficiency of signal detection. In broadband communication systems, noise may cause the noise floor of the signal power spectrum to be unstable, which requires accurate identification and differentiation of signals and noise through noise floor estimation [16, 17]. However, the traditional method of calculating the average bottom noise power is difficult to accurately estimate the noise level when the noise base is uneven, resulting in an increase in the missed detection rate of signal detection. Therefore, research is based on DCAE to estimate the signal noise floor. The process is shown in Fig. 3.

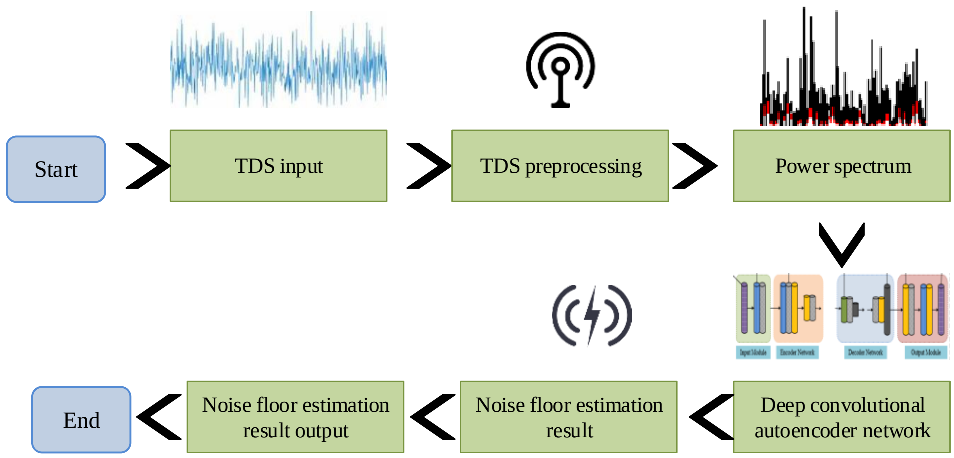

Figure 3: Schematic diagram of the noise bottom estimation method based on DCAE

As shown in Fig. 3, firstly, the time-domain signal (TDS) to be processed is input into the system. This signal may contain noise and useful information. Then the input TDS is preprocessed to enhance the effectiveness and precision of subsequent processing. The preprocessing steps include filtering, denoising, normalization, and other operations. Then, the preprocessed TDS is converted to the frequency domain, and Welch is sampled to calculate its power spectrum. The power spectrum reflects the power distribution of a signal at different frequencies. The calculated power spectrum is further input into DCAE. This network extracts features and denoises the power spectrum through convolutional and deconvolution layers to estimate the noise floor. Ultimately, the noise floor estimation outcomes are output for subsequent signal processing or analysis. Welch's calculation of the power spectrum of broadband communication signals is shown in equation (4).

$$P_{Welch}(m) = \frac{1}{K}\sum_{k=1}^{K}\frac{1}{U}|X_k(m)|^2 \quad (4)$$

In equation (4), K is the number of segments. U is the normalization factor for the window function. $X_k(m)$ is the result of the discrete Fourier transform of the k th segment signal. The results are further normalized. The noise floor estimation result of the final input power spectrum is shown in equation (5).

$$Y = \tilde{Y}(\max(I) - \min(I)) + \min(I)) \quad (5)$$

In equation (5), Y is the normalized value. $\tilde{Y}$ is the value of the original data. I is the entire collection of raw data.

3.2 Communication signal detection based on SCN

The research focused on the estimation of the noise floor for communication broadband signals utilizing the DCAE approach. Through automatic learning and extraction of noise features, DCAE can accurately estimate the noise floor, providing a foundation for signal detection. However, noise floor estimation is only a part of signal detection, and in order to achieve complete communication signal detection, further research is needed to identify useful communication signals. However, traditional communication signal detection methods have multiple limitations in terms of anti-interference ability, adaptability, automation level, and the trade-off between complexity and performance. These limitations are particularly evident in complex electromagnetic environments and low SNR conditions, which affect the accuracy and reliability of signal detection [18, 19]. The core idea of SCN is to treat the Broadband Power Spectrum Sequence (BPS) as a one-dimensional image and each sub-carrier on the broadband as the target object, thereby transforming the carrier signal detection problem into a semantic segmentation problem on a one-dimensional image [20]. However, due to the large length of the power spectrum of broadband communication signals, it is difficult to match the image. Therefore, research is being conducted to improve the deep Residual Backbone Network (ResNet backbone) in the SCN model and detect communication signals based on the optimized SCN. The optimized SCN model structure diagram is shown in Fig. 4.

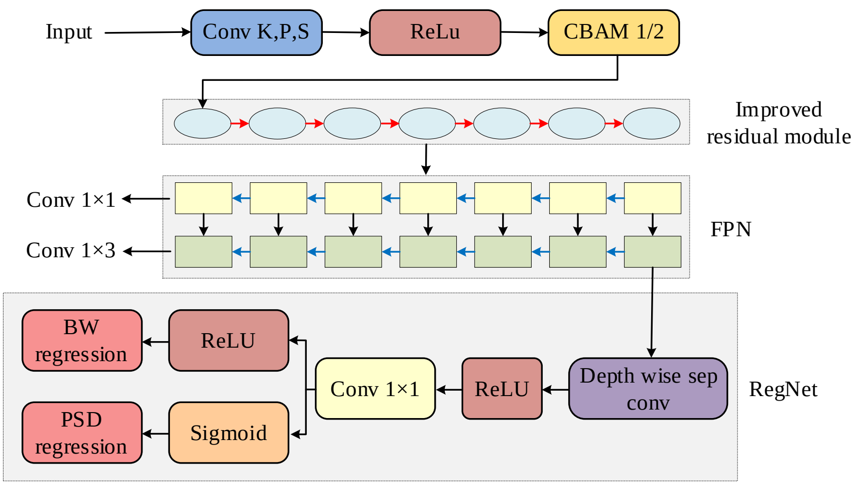

Figure 4: Structural diagram of the SCN model

As shown in Fig. 4, the SCN is mainly composed of three parts. The improved deep residual backbone network (ResNet) utilizes residual blocks and skip connections to effectively solve the problem of gradient vanishing in deep network training, enhancing the model's ability to learn complex signal features. Feature Pyramid Network (FPN) improves the detection performance of carrier signals by constructing a top-down information flow and combining horizontal connections to fuse high-level semantic information with low-level spatial information. Regulated Network (RegNet) parameterizes the width and depth of the network through quantized linear functions, and the optimized network structure improves the accuracy of frequency center and bandwidth prediction. The overlapping of adjacent carrier frequency edges can lead to a reduction in the frequency gap of the signal power spectrum, thereby affecting the accuracy of feature extraction in SCNs. The study dynamically adjusted the feature response of each channel by embedding the Squeeze and Excitation Net (SENet) module after the convolutional layer, further improving the detection accuracy. These improvements enable SCN to perform well in complex electromagnetic environments, enabling more accurate identification of carrier signals and demonstrating higher robustness and adaptability compared to traditional methods. The SENet structure is in Fig. 5.

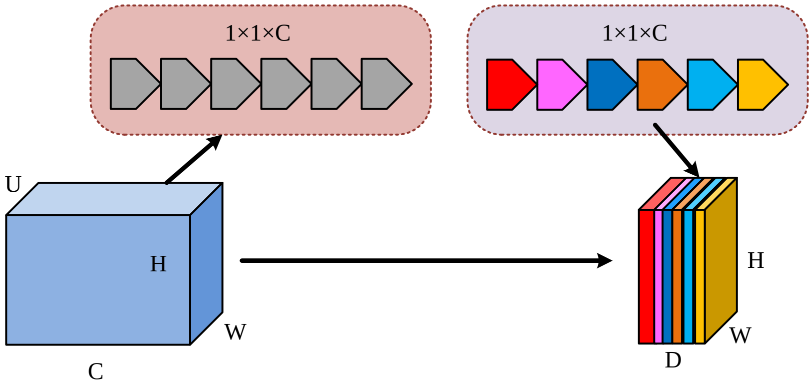

Figure 5: Illustration of the SENet module structure

As shown in Fig. 5, The SENet module consists of two main operations: squeeze and excitation. Firstly, the SENet module compresses the spatial dimension of each channel in the input feature map through global average pooling operation, thereby obtaining the global description of each channel. Next, the SENet module utilizes a self gating mechanism consisting of two fully connected layers and a nonlinear activation function to generate weights for each channel. These weights reflect the importance of each channel, allowing the model to dynamically adjust the level of attention given to different channels. Finally, the SENet module applies the generated weights to the original feature map, re-calibrates each channel, enhances the model's focus on key features, and improves the accuracy of feature extraction. Through this mechanism, the SENet module can effectively address the challenges posed by reducing frequency gaps and improve the detection performance of the model in complex electromagnetic environments. The calculation of the dimensionality enhancement layer is shown in equation (6).

$$s_i = \sigma(Ws_i^{'} + y) \quad (6)$$

In equation (6), s_i represents the final channel weight, W and y represent the weight and bias of the FCL. $s_i^{'}$ is the output of the dimensionality reduction layer. σ is a non-linear AF. The specific calculation of global average pooling is shown in equation (7).

$$z_i = \frac{1}{H \times W} \sum_{u=1}^{H} \sum_{v=1}^{W} F_{i,u,v} \quad (7)$$

In equation (7), z_i is the global average pooling result of the i th channel. H and W are the height and width of the feature map. $F_{i,u,v}$ is the value of the input feature map F in the i th channel, u th row, and v th column. Usually, after the second FCL, a Sigmoid AF serves to guarantee that the output weights lie within the range of 0 and 1, which can effectively recalibrate the channels of the original feature map. The specific calculation is shown in equation (8).

$$s_i = \mathrm{Sigmoid}(W_2 \sigma(W_1 z_c + y_1) + y_2) \quad (8)$$

In equation (8), W_1, y_1, W_2, and y_2 are the WM and bias vector of the FCLs in the first and second layers, respectively. The communication signal detection process based on SCN is in Fig. 6.

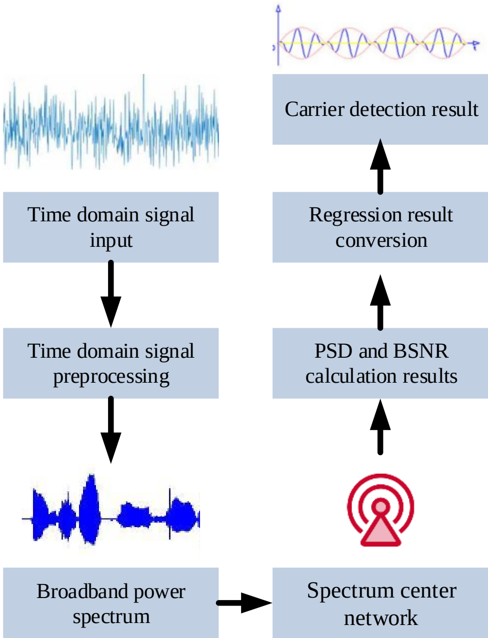

Figure 6: Flow chart of communication signal detection based on SCN

In Fig. 6, the first step is the input and preprocessing of TDSs. The preprocessed signal is converted to the frequency domain to generate a BPS. Then, the BPS is input into the SCN for identifying and locating carrier signals in the power spectrum. In the SCN, ResNet is responsible for extracting features of different length scales, the FPN is responsible for fusing features and outputting them, RegNet predicts frequency centers and bandwidths, and detects subcarrier targets through non maximum suppression. Finally, the SCN outputs the estimation results of power spectral density and bandwidth. These results are then utilized for regression conversion, which ultimately yields the final carrier detection outcome.

4 Results

4.1 Testing conditions and configuration settings

To verify the performance of communication signal detection methods based on DCAE and SCN, the study was conducted on the Ubuntu 20.04 LTS operating system experimental platform. From a hardware perspective, the selection of the GeForce RTX 3080Ti GPU stemmed from its exceptional computational prowess and substantial video memory capacity. These attributes enabled it to effectively manage training tasks associated with intricate models like DCAE networks. However, its high-power consumption and heat dissipation requirements limited the flexibility of the experimental environment, and an efficient heat dissipation system must be equipped to ensure stable operation. Paired with Intel (R) Bronze 3204 CPU, its multi-threaded processing capability can meet the needs of data preprocessing and model evaluation; 64 GB of memory can handle large-scale datasets. In terms of software, although the Ubuntu 20.04 LTS operating system is stable and highly compatible, its Linux-based features require users to have certain command line operation skills. By utilizing the PyTorch 1.10.0 deep learning framework, which is celebrated for its dynamic computation graphs, intuitive design, and the extensive array of community-provided resources, a robust platform was established. Nevertheless, for particular specialized tasks, it may be essential to conduct further code optimization or incorporate additional tools, such as Horovod, to achieve efficient parallel computing. The specific parameter configuration of the experiment environment is shown in Table 1.

Table 1 Setting of the experiment environment

	Configure	Model/version
Hardware configuration	CPU	GeForce RTX 3080Ti
	GPU	Intel(R) Bronze 3204
	Storage	64 GB

Software configuration	Operating system	Ubuntu 20.04 LTS
	DL framework	And PyTorch1.10.0 based on the Python language
SCN parameter Settings	Model input length	32,768
	Batch size	32
	Optimizer	Adam

The process of selecting hyper-parameters for the experiment was as follows. The batch size was determined based on the balance between training speed and generalization ability, and was selected after testing multiple values through experiments. The learning rate adopted a combination of grid search and random search to find the optimal value within the range of 0.001 to 0.1. Dropout rate was determined by testing different ratios and selecting values that effectively prevented overfitting without affecting performance. The network structure of the DCAE-SCN model in the study consisted of an encoder and a decoder, each containing three convolutional and deconvolution layers, with a kernel size of 3x3 and a stride of 1. The encoder normalized and prevented overfitting through Batch Normalization and Dropout, while the decoder used ReLU activation function. In terms of computational complexity, the average inference time of the DCAE model was 0.025s, which was slightly longer than the 0.015s of the ED method, but the detection performance was significantly better. Similar to the 0.03s of DLD method, the performance was better. Sensitivity analysis of model parameters was conducted in the experiment, including learning rate, batch size, and dropout rate. The results showed that when the learning rate was set to 0.01, the model achieved the highest detection accuracy of 98.5%, indicating that a moderate learning rate helped the model learn effectively. When the batch size was 64, the model performed the best with a detection accuracy of 98.1%, indicating that a moderate batch size was helpful for stable training of the model. When the Dropout rate was 0.3, the model accuracy was the highest at 98.5%, indicating that an appropriate Dropout rate could effectively prevent overfitting and improve the model's generalization ability. The experiment trained a communication signal detection method based on DCAE and SCN, using a dataset of real signal samples with a total of 10000 samples, including 7000 for training, 2000 for validation, and 1000 for testing. The model training went through 50 iteration cycles, with each cycle performing forward and backward propagation on all training samples.

4.2 Performance analysis of communication signal detection methods

To verify the performance of DCAE, a Dropout layer was added in the experiment, and model scales of 1, 5, and 10 were selected for comparative experiments. The model size refers to the number of convolutional and deconvolution layers in DCAE, covering network structures from simple to complex on three scales. For example, model scale 1 indicates that there is only one convolutional layer and one deconvolution layer in the network, which is the simplest structure with low computational complexity. By selecting network structures of different depths, the impact of model complexity on detection performance can be evaluated. The results from the experiment are depicted in Fig. 7.

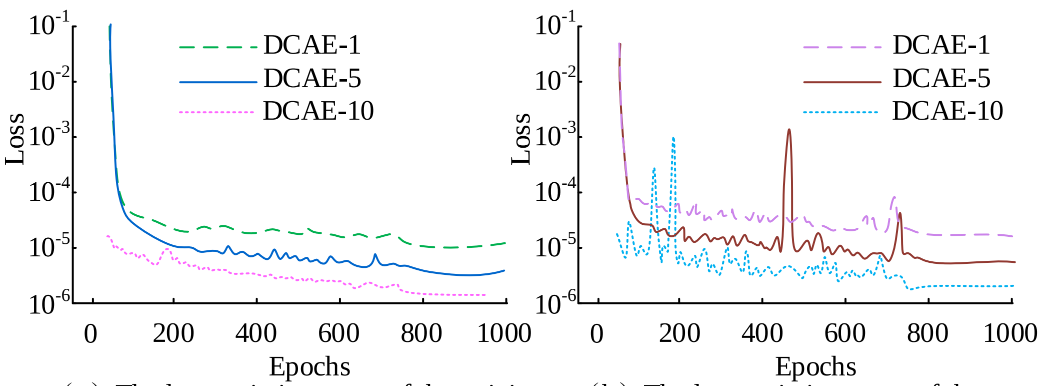

（a）The loss variation curve of the training set （b）The loss variation curve of the validation set

Figure 7: DCAE training process loss change curve

Figs. 7 (a) and (b) show the variation curves of the loss function of the DCAE function on the training and validation sets, respectively. The loss function was normalized to mean squared error (MSE), therefore its values were in dimensionless units. As the number of training rounds increased, the loss values of the functions at all three model scales gradually decreased, with a decreasing trend of first fast and then slow, and then gradually stabilizing. As shown in Fig. 7 (a), the loss values of DCAE-1 and DCAE-5 models decreased rapidly, and their relative stable loss function values were both around 10-5. The initial loss value of DCAE-10 was the lowest, the loss value decreased the slowest, and the minimum loss function value was about 10-6. As shown in Fig. 7 (b), the functions of the three model scales gradually stabilized after 750 training iterations, with DCAE-1 having the highest loss function value when stable, followed by DCAE-5, and DCAE-10 having the lowest. The experimental results showed that none of the three loss functions exhibited overfitting, indicating that the loss function had good performance. To verify the feasibility of the broadband communication signal detection method based on DCAE and SCN proposed by the research, ED and DLD were selected for comparative experiments. The experiment tested the differences in detection performance of various algorithms under different SNR conditions. The obtained results are shown in Fig. 8.

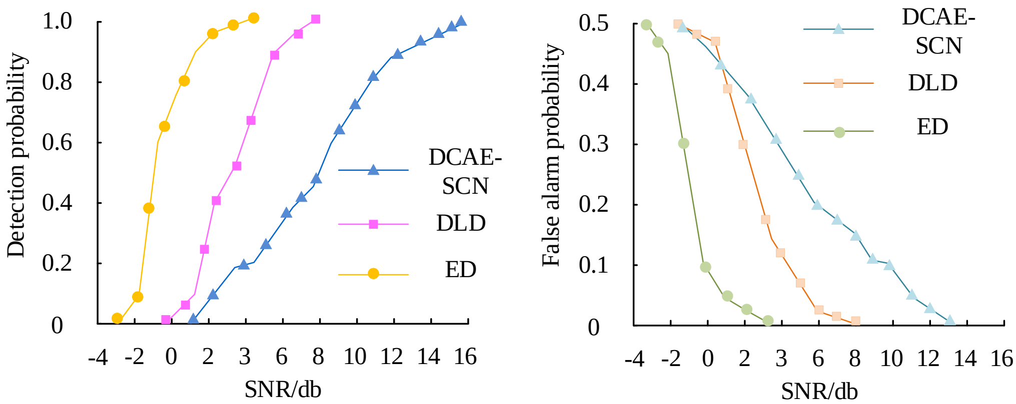

（a）Comparison of detection probabilities

（b）Comparison of False alarm probabilities

Figure 8: Performance comparison diagram of each signal detection method

Figs. 8 (a) and (b) show the detection probability (DP) and false alarm probability (FAP) of each signal detection method, respectively. As shown in Fig. 8 (a), the DP of each signal detection method gradually increased with the increase of SNR. When the DP was 0, the SNRs of DCAE-SCN, DLD, and ED were -3db, 0db, and 1db, respectively. The DP of the three signal detection methods reached its maximum value of 1 when the SNR was 16db, 8db, and 3db, respectively. As shown in Fig. 8 (b), the FAP of each signal detection method gradually decreased with the increase of SNR. When the FAP of DCAE-SCN, DLD, and ED was 0, the SNRs were 13db, 8db, and 3db, respectively. Overall, the DCAE-SCN method performed the best in both DP and FAP, followed by DLD and ED. This may be due to the DCAE-SCN method adopting a more complex model structure and optimization algorithm, which enabled it to more effectively extract features and reduce noise impact when processing signals, thus exhibiting higher DP and lower FAP under various SNR conditions. The feature extraction ability of DLD and ED methods may be relatively weak, especially under low SNR conditions, making it difficult to effectively distinguish between signals and noise, resulting in a lower DP. To further confirm the stability of the raised communication signal detection method, different Interference-to-Signal Ratio (ISR) conditions were set up in the experiment, and different communication signal detection methods were used for signal detection experiments. The specific results obtained are shown in Fig. 9.

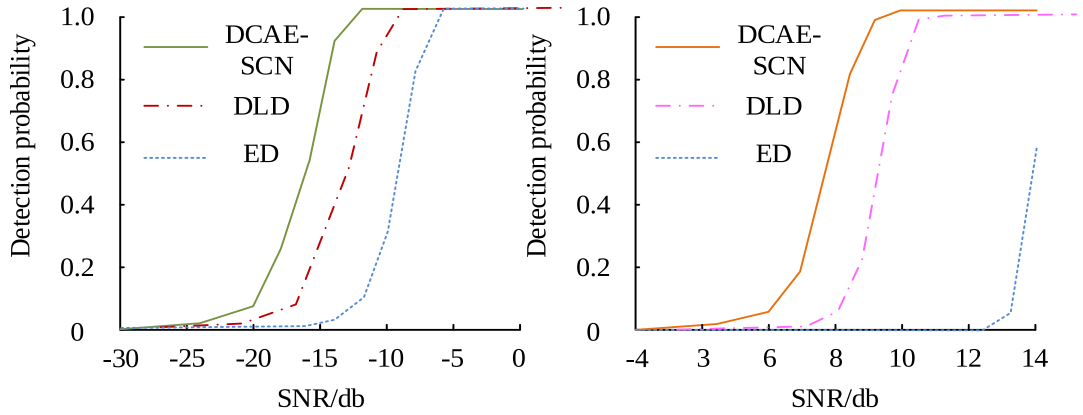

（a）Detection probability when the SNR is -10db （b）Detection probability when the SNR is 0db

Figure 9: Results plot of DP of each test method under ISR at different methods

Figs. 9 (a) and (b) show the DPs of each signal detection method at ISR levels of -10db and 0db, respectively. From Fig. 9 (a), the DPs of each signal detection method showed an upward trend with the increase of ISR, and the rate of change was first fast and then slow. After the DP reached 1, it no longer changed. DCAE-SCN reached a stable state as quickly as possible, with an ISR of -13db. DLD and ED reached stability at around -11db and -6db, respectively. As shown in Fig. 9 (b), DCAE-SCN exhibited a rapid increase in DP and approached 1 when the SNR was greater than 2db, demonstrating superior performance in medium SNR environments. When the SNR was greater than 4db, the DP of DLD increased rapidly. When the SNR was greater than 6db, the DP of ED started to significantly increase, and reached its maximum value of 0.6 at 14db. Overall, DCAE-SCN performed the best in DP under various SNR environments, followed by DLD, and the ED method performed the worst. DCAE-SCN may have undergone more refined parameter tuning and comprehensive experimental design, enabling the algorithm to achieve optimal performance under various SNR conditions. Although the performance of DLD was not as good as DCAE-SCN, its DP rapidly increased when the SNR was greater than 4db, indicating that this method had certain feature extraction and noise suppression capabilities under moderate SNR conditions, but might not be as comprehensive or optimized as DCAE-SCN. The ED method had weak feature extraction and noise suppression capabilities under low and medium SNR conditions, possibly due to a simple algorithm design or insufficiently complex models. The experiment further validated the detection probability of the communication signal detection method proposed by the research under different code length signal conditions. The specific results obtained are shown in Fig. 10.

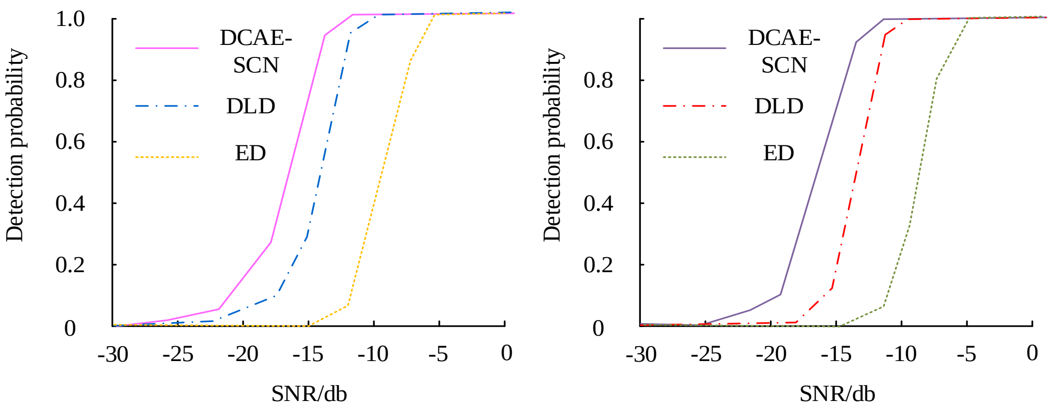

（a）Detection performance of signals with different code lengths （b）Detection performance under color noise

Figure 10: Comparison diagram of the detection performance of each signal detection method

Fig. 10 (a) shows the DPs of various methods for signals of different code lengths, and Fig. 10 (b) shows the DPs of various methods for communication signals under different colored noise backgrounds. As shown in Fig. 10

(a), the DP of DCAE-SCN rapidly increased with the increase of SNR, and the DP was 1 at an SNR of -16db. The probability of DLD detection started to increase when the SNR was greater than -20 db, and approached 1 when the SNR was -10 db. The probability of ED detection started to increase when the SNR was greater than -25db, but the rate of increase was slow and did not reach 1 when the SNR reached 0db. As shown in Fig. 10 (b), DCAE-SCN, DLD, and ED reached their maximum DPs at SNRs of -16db, -12db, and -6db, respectively, and did not change thereafter. DCAE-SCN performed well in different colored noise backgrounds, indicating that it may have had better noise modeling and suppression capabilities, and could effectively distinguish between signals and noise. The slow performance improvement of the DLD and ED methods in different colored noise backgrounds may have indicated their limited ability to handle non-Gaussian or correlated noise. To evaluate the importance of different components in the DCAE-SCN model, ablation experiments were conducted, and the results are shown in Table 2.

Table 2: DCAE-SCN ablation experiment data table

Model configuration	Detection accuracy (%)	F1	Recall (%)	Detection tim (s)
DCAE-SCN	98.5 ± 0.4	0.99	0.98	0.025
No SENet	97.0 ± 0.5	0.98	0.96	0.023
No convolutional layer	92.0 ± 0.6	0.94	0.91	0.021
No deconvolution layer	95.0 ± 0.5	0.96	0.94	0.024
Reduce the number of convolutional layers (5 layers)	96.5 ± 0.4	0.97	0.95	0.022
Reduce the number of deconvolution layers (5 layers)	96.0 ± 0.5	0.96	0.94	0.022

According to Table 2, in the complete DCAE-SCN model, the detection accuracy reached 98.5%, the F1 value was 0.99, the recall rate was 98%, and the detection time was 0.025 seconds, demonstrating the high accuracy and efficiency of the model. When the SENet module was removed, the detection accuracy dropped to 97.0%, indicating that SENet played an important role in improving model performance, possibly by enhancing feature selectivity to improve the model's generalization ability. Further removal of convolutional layers resulted in a significant decrease in accuracy to 92.0%, highlighting the importance of convolutional layers in extracting key features. The removal of the deconvolution layer also led to a decrease in performance, but the impact was relatively small, with an accuracy of 95.0%, which might be because the model could still learn some features through the remaining structure. Reducing the number of convolutional and deconvolution layers also led to a performance degradation of 96.5% and 96.0%, respectively, which validated the necessity of deep structures for learning complex features. These results indicated that each part of the model contributed to the final performance, especially the crucial role of convolutional layers in feature extraction and the importance of SENet modules in improving the model's generalization ability. To verify the robustness of the proposed method under adversarial noise conditions, experiments were conducted to test the performance of each algorithm under four different types of noise: uniform noise, impulse noise, salt and pepper noise, and speckle noise, as well as narrowband interference and broadband interference. The obtained results are shown in Fig. 11.

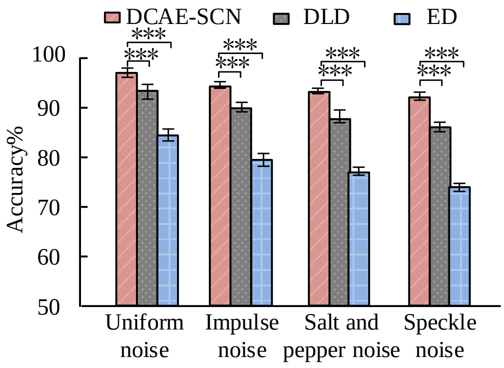

(a) Accuracy of the next algorithm under different types of noise

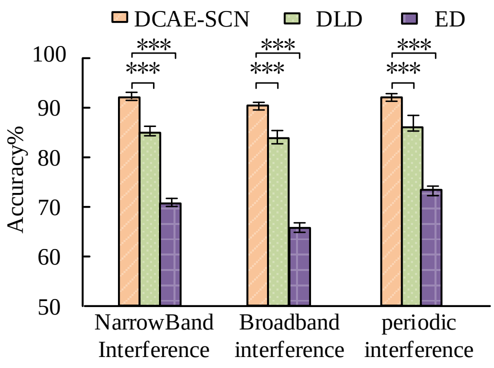

(b) Accuracy of the next algorithm under different types of interference

Figure 11: Performance comparison results of different algorithms under adversarial noise conditions

Note: * * * indicates that the difference is statistically significant, *p*<0.01.

As shown in Fig. 11 (a), under uniform noise and impulse noise conditions, the DCAE-SCN algorithm had the highest accuracy, approaching 95% and 90% respectively, demonstrating its superior performance in handling these noises. In contrast, the ED algorithm had lower accuracy under these two types of noise, especially under impulse noise, where the accuracy dropped to about 80%. Salt and pepper noise, as well as speckle noise, posed challenges to all algorithms, but DCAE-SCN still maintained relatively high accuracy rates of 90% and 92%, respectively. This might be due to DCAE-SCN's ability to better learn noise patterns and effectively suppressed them. As shown in Fig. 11 (b), under narrowband interference and broadband interference conditions, DCAE-SCN still had the highest accuracy, about 90% and 85% respectively, indicating its advantage in handling spectrum selective interference. The impact of periodic interference on all algorithms was relatively small, but DCAE-SCN still led with an accuracy of about 90%. The performance of DLD algorithm was inferior to DCAE-SCN under all interference conditions, while ED algorithm performed the worst under broadband interference, with accuracy dropping to about 65%. This might be because ED algorithm was difficult to adapt to the spectral characteristics of broadband interference. To verify the robustness of the proposed algorithm in practical situations, further experiments were conducted to test the signal detection performance of each method in real electromagnetic environments. The specific results obtained are shown in Table 3.

Table 3: Performance comparison outcomes of each test method

Testing environment	Laboratory environment			Real electromagnetic environment		
Test method	DCAE-SCN	DLD	ED	DCAE-SCN	DLD	ED
Detection accuracy (%)	98.5 ± 0.4	93.2 ± 0.5	85.0 ± 0.6	97.2 ± 0.4	92.0 ± 0.5	82.5 ± 0.7
Confidence interval (test accuracy)	[98.1, 98.9]	[92.7, 93.7]	[84.4, 85.6]	[96.8, 97.6]	[91.5, 92.5]	[81.8, 83.2]
F1	0.99	0.95	0.88	0.98	0.94	0.85
Recall (%)	0.98	0.94	0.82	0.97	0.93	0.81
Detection tim (s)	0.025	0.030	0.015	0.025	0.030	0.015

According to Table 3, the detection accuracy of DCAE-SCN method in laboratory environment was 98.5%, F1 value was 0.99, and recall rate was 0.98, demonstrating its superior performance under ideal conditions. In contrast, the detection accuracies of DLD and ED methods were 93.2% and 85.0%, respectively, with F1 values of 0.95 and 0.88, and recall rates of 0.94 and 0.82, respectively, both lower than DCAE-SCN. This indicated that DCAE-SCN was more effective in feature extraction and signal recognition, especially when dealing with complex signals. In the real electromagnetic environment, the detection accuracy of DCAE-SCN slightly decreased to 97.2%, but it was still higher than DLD (92.0%) and ED (82.5%). This might be due to the more complex signal interference and noise in real environments, but DCAE-SCN better adapted to these changes through its DL architecture. The detection time of DCAE-SCN was 0.025 seconds in both environments, demonstrating its excellent real-time performance while maintaining high detection performance. The confidence interval provided statistical validity for the detection accuracy. The standard error of DCAE-SCN in both environments was 0.4%, with confidence intervals of [98.1, 98.9] and [96.8, 97.6], indicating that the estimation of its detection accuracy was stable and reliable. The standard error of DLD method was relatively large at 0.5%, but its performance in two environments also showed good stability. In contrast, the standard error of the ED method under laboratory and real conditions was 0.6% and 0.7%, respectively, indicating that its results fluctuated greatly and its reliability was relatively low. Overall, DCAE-SCN exhibited high robustness and accuracy in different environments, validating its effectiveness as an advanced detection method. Although the ED method had the shortest running time, it was not as accurate and robust as DCAE-SCN, possibly due to the limitations of its algorithm in processing complex signals. The DLD method had the longest detection time, possibly due to its algorithm or implementation efficiency not being as optimized as DCAE-SCN.

5 Discussion

The proposed method based on DCAE and SCN signal noise floor estimation and communication signal detection achieved significant improvements in multiple key performance indicators. Firstly, DCAE-SCN, through its DCAE network structure, utilized convolutional and deconvolution layers to effectively capture multi-level features of signals. Secondly, under low SNR conditions, signals were often overwhelmed by noise, and traditional methods might experience performance degradation due to their inability to effectively extract signal features. The SENet module in DCAE-SCN's network architecture could dynamically adjust feature responses, enhance the model's attention to key features, and thus improve detection accuracy.

In terms of computational cost, DCAE-SCN had a certain increase in computational complexity compared to simpler signal detection methods. Although the computational complexity increased, DCAE-SCN ensured that its inference time was still relatively short by optimizing the network structure and training process, which could meet the requirements of real-time communication systems. Compared with other DL methods such as DLD, DCAE-SCN further optimized computational efficiency by introducing improvement measures such as SENet while maintaining high performance.

From the perspective of practical deployment, DCAE-SCN had a high feasibility in real-time communication systems. Its moderate computational complexity and short inference time enabled it to operate in resource constrained environments, while its high detection accuracy and robustness ensured reliable operation of the system in complex electromagnetic environments. In addition, the DL architecture of DCAE-SCN allowed it to adapt to different communication scenarios and signal types through further training and optimization.

6 Conclusion

With the swift advancement of information technology, communication systems are becoming increasingly crucial in various fields of society. To develop a new signal detection method to improve detection accuracy in complex electromagnetic environments and low SNR conditions, the study proposed a communication signal detection method based on DCAE and utilized SCN for carrier signal detection. The experiment outcomes indicated that when the DP was 0, the SNRs of DCAE-SCN, DLD, and ED were -3db, 0db, and 1db, respectively. The three signal detection methods had a maximum DP of 1 when the SNR was 16db, 8db, and 3db, respectively. When the FAP of DCAE-SCN, DLD, and ED was 0, the SNRs were 13db, 8db, and 3db, respectively. Under the DP condition of -10db ISR, the DPs of each signal detection method showed an upward trend with the increase of ISR, and their change rate was fast at first and then slowed down. After the DP reached 1, it no longer changed. DCAE-SCN reached a stable state as quickly as possible, with an ISR of -13db. DLD and ED reached stability at around -11db and -6db, respectively. The experiment showed that this method outperformed the ED and DLD methods in performance indicators such as detection accuracy, F1 value, and recall, providing an effective solution for communication signal detection within intricate electromagnetic surroundings. However, the research was mainly conducted in specific datasets and experimental environments, without exploring the generalization ability of the method in unknown environments or data. Therefore, future research will increase the diversity and complexity of training data to enhance the model's generalization ability to signals in different environments and conditions, in order to enable it to play a greater role in a wider range of application scenarios. In addition, future work can focus on optimizing model structures, improving robustness to non Gaussian noise, and applying this technology to interdisciplinary fields such as radar signal processing and biomedical signal analysis to expand its application scope and deepen theoretical research. Future endeavors could also delve into integrating emerging technologies, like quantum computing, to further enhance the precision and efficiency of signal detection.

Data availability statement

All data generated or analysed during this study are included in this article.

Conflict of interest

The authors declare that they have no competing interests.

Funding statement

There is no funding in this article.

References

[1] Saikia P, Biswas S, Singh K. Signal detection in GSm-based in-band full-duplex communication using DNN. IEEE Trans. Veh. Technol., 2023, 72(2): 2661-2666. https://doi.org/10.1109/TVT.2022.3211652

[2] Zhang Y, Pan Y, Gong C. Channel estimation and signal detection for nlos ultraviolet scattering communication with space division multiple access. IEEE Trans. Commun., 2024, 72(10): 6427-6441. https://doi.org/10.1109/TCOMM.2024.3400917

[3] Yu W, Liu F, Yan H. Evaluation of non-coherent signal detection techniques for mobile molecular communication. IEEE Trans. Nanobiosci., 2023, 22(2): 356-364. https://doi.org/10.1109/TNB.2022.3193392

[4] Miki Y, Kobayashi K, Chujo W. Data signal detection and demodulation based on object detection DNN for image sensor-based visible light communication. IEICE Commun. Express, 2023, 12(12): 628-632. https://doi.org/10.23919/comex.2023XBL0105

[5] Liu H, Liu X. Intelligent detection and search model for communication signals based on deep-re-hash retrieval technology. Int. J. Adv. Comput. Sci. Appl., 2024, 15(9): 824-835. https://doi.org/10.14569/IJACSA.2024.0150984

[6] Xiao L, Rao X, He W. Weak target integration detection based on radar communication integrated signal via constructed Step-LFM model. Radioengineering, 2024, 33(1): 195-203. https://doi.org/10.13164/re.2024.0195

[7] Jiang X, Diao M. A new type double-threshold signal detection algorithm for satellite communication systems based on stochastic resonance technology. Wirel. Netw., 2024, 30(5): 3367-3374. https://doi.org/10.1007/s11276-019-02020-8

[8] Li S, He D, Wang W, You M. A stochastic resonance detection method for broadband communication signals in small loads. J. Signal Process., 2024, 40(4): 671-681. https://doi.org/10.16798/j.issn.1003-0530.2024.04.006

[9] Chen Y, Khuwaja A A, Wang C. Effect of source signal traffic on signal detection for ambient backscatter communication. IEEE Trans. Veh. Technol., 2024, 73(11): 16790-16804. https://doi.org/10.1109/TVT.2024.3419423

[10] Liu Z, Zhao Q, Xu L. Preamble signal detection method of underwater acoustic communication based on lightweight convolutional neural network. J. Signal Process., 2023, 39(10): 1831-1841. https://doi.org/10.16798/j.issn.1003-0530.2023.10.010

[11] Arya S, Chung Y H. Fault-tolerant cooperative signal detection for petahertz short-range communication with continuous waveform wideband detectors. IEEE Trans. Wireless Commun., 2023, 22(1): 88-106. https://doi.org/10.1109/TWC.2022.3191322

[12] Bai C, Zhu A, Lu X. Temporal convolutional network-based signal detection for magnetotactic bacteria communication system. IEEE Trans. Nanobiosci., 2023, 22(4): 943-955. https://doi.org/10.1109/TNB.2023.3262555

[13] Byun H. Adaptive signal detection method using distance estimation for diffusion-based nanosensor communication systems. IEEE Sensors J., 2024, 24(3): 3703-3710. https://doi.org/10.1109/JSEN.2023.3342805

[14] Cheng Z, Zhang Z, Sun J. Signal detection of cooperative multi-hop mobile molecular communication via diffusion. IEEE Trans. Mol. Biol. Multi-Scale Commun., 2024, 10(1): 101-111. https://doi.org/10.1109/TMBMC.2024.3360341

[15] Xu X, Huang T, Kuai X. Joint localization and signal detection for ambient backscatter communication systems. IEEE Trans. Wireless Commun., 2024, 23(10): 14437-14451. https://doi.org/10.1109/TWC.2024.3414119

[16] Ke D, Wang X, Huang K, Liu H, Guo Y. Minimum power adversarial attacks in communication signal modulation classification with deep learning. Cognit. Comput., 2023, 15(02): 580-589. https://doi.org/10.1007/s12559-022-10062-y

[17] Shoukat H, Khurshid A A, Daha M Y. A Comparative analysis of DNN and conventional signal detection techniques in SISO and MIMO communication systems. Telecom, 2024, 5(2): 487-507. https://doi.org/10.3390/telecom5020025

[18] Zheng Y, Tu X. Target signal communication detection of black flying UAVs based on deep learning algorithm. Recent Adv. Comput. Sci. Commun., 2024, 17(8): 52-61. https://doi.org/10.2174/012666255826832123123106 5419

[19] Wang Y, Song L. Application and optimization of convolutional neural networks based on deep learning in network traffic classification and anomaly detection. Informatica, 2025, 49(14). https://doi.org/10.31449/inf.v49i14.7602

[20] Li L, Dong Z, Zhu Z, Guo W, Zhang B, Song H. Deep-learning hopping capture model for automatic modulation classification of wireless communication signals. IEEE Trans. Aerosp. Electron. Syst., 2023, 59(02): 772-783. https://doi.org/10.1109/TAES.2022.3189335